Small-Angle X-ray Scattering Investigations of Biomolecular Confinement, Loading, and Release from Liquid-Crystalline Nanochannel Assemblies

ARTICLE *in* JOURNAL OF PHYSICAL CHEMISTRY LETTERS · FEBRUARY 2012

Impact Factor: 7.46 · DOI: 10.1021/jz2014727

6 AUTHORS, INCLUDING:

Angelina Angelova
Université Paris-Sud 11
88 PUBLICATIONS **1,667** CITATIONS
SEE PROFILE

Borislav Angelov
Academy of Sciences of the Czech Republic
51 PUBLICATIONS **937** CITATIONS
SEE PROFILE

Vasil M Garamus
Helmholtz-Zentrum Geesthacht
223 PUBLICATIONS **2,528** CITATIONS
SEE PROFILE

Patrick Couvreur
Université Paris-Sud 11
581 PUBLICATIONS **25,694** CITATIONS
SEE PROFILE

THE JOURNAL OF PHYSICAL CHEMISTRY Letters

Perspective

pubs.acs.org/JPCL

Small-Angle X-ray Scattering Investigations of Biomolecular Confinement, Loading, and Release from Liquid-Crystalline Nanochannel Assemblies

Angelina Angelova,*[,†] Borislav Angelov,[‡] Vasil M. Garamus,[§] Patrick Couvreur,[†] and Sylviane Lesieur[†]

[†]CNRS UMR8612 Physico-chimie-Pharmacotechnie-Biopharmacie, Univ Paris Sud 11, Châtenay-Malabry, F-92296 France

[‡]Institute of Macromolecular Chemistry, Academy of Sciences of the Czech Republic, 16206 Prague, Czech Republic

[§]Helmholtz-Zentrum Geesthacht, Centre for Materials and Coastal Research, 21502 Geesthacht, Germany

ABSTRACT: This Perspective explores the recent progress made by means of small-angle scattering methods in structural studies of phase transitions in amphiphilic liquid-crystalline systems with nanochannel architectures and outlines some future directions in the area of hierarchically organized and stimuli-responsive nanochanneled assemblies involving biomolecules. Time-resolved small-angle X-ray scattering investigations using synchrotron radiation enable monitoring of the structural dynamics, the modulation of the nanochannel hydration, as well as the key changes in the soft matter liquid-crystalline organization upon stimuli-induced phase transitions. They permit establishing of the inner nanostructure transformation kinetics and determination of the precise sizes of the hydrophobic membraneous compartments and the aqueous channel diameters in self-assembled network architectures. Time-resolved structural studies accelerate novel biomedical, pharmaceutical, and nanotechnology applications of nanochannel soft materials by providing better control of DNA, peptide and protein nanoconfinement, and release from diverse stimuli-responsive nanocarrier systems.

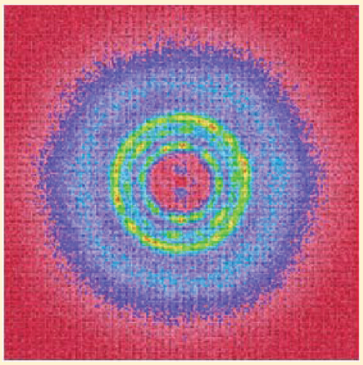

Confinement and transport of biomolecules in and through constrained geometries, such as nanochannels and nanopores, has been an exciting topic in nanotechnology.[1−28] Open-channel architectures exist in various spatial organizations[4,10,29−56] and are significant for both conducting biological functions and fabrication of nanochanneled advanced functional or biomimetic materials. The channel sizes are allowed to scale between two extremities represented by single channel-forming systems[3,4,29−31] and channel-making hierarchical colloidal systems[41] (Figure 1). The channel diameter can span from Ångströms to micrometers, the nanometer size channel structures being the most advantageous for biomedical, pharmaceutical, and functional food innovations.[15−17,57−67]

Among the molecular channel systems, membrane channel proteins[3,4,29−31] have been widely investigated in nanotechnology as they can be incorporated into lipid bilayers or in reconstituted biomimetic polymer membranes at a controllable channel density. This permits the fabrication of highly permeable and ion-selective membrane architectures.[3,29,30] Each transmembrane channel protein may represent a switchable, stimuli-responsive channel (Figure 1A). The diameters of the transmembrane protein channels have been estimated in the range from 0.3 to 3.8 nm. The size of the pores can be extended up to 5 nm with some channel proteins.[29−31] Transmembrane protein channels and pore proteins display a capacity for reversible channel switching and unidirectional transport of ions and molecules. Their ligand gating,ion-selective, and pore-forming properties have attracted considerable interest for biosensor and nanomedical applications.[30]

At the opposite extremity of channel sizes, the micrometer-scale assemblies of nanoparticles (NPs) and vesicles[2,41] are also generating channel structures and channel networks. This comes into the field of hierarchical self-assembly, which has shown tremendous growth during the recent years.[2,27,28,37−42,47] Hierarchical self-assembly can produce either soft, stimuli-responsive channel structures with tunable diameters[7−9,15,34−36] or solid networks with fixed channel diameters.[39,40] The network of polymersomes (polymer vesicles), created by a pH-triggered multilevel self-recognition process,[41] is an example of such a colloidal system with soft channels (Figure 1K).

In between these two limits of channel sizes, one can situate the natural biological and biomimetic nanochannel architectures formed by self-assembled proteins in viral NPs[32] (see, for instance, the CCMV capsid in Figure 1B). Helical nanochannel assemblies have been created by biomimetism employing intermolecular H-bonding interactions between oligopeptide macrocycles[42] (Figure 1J). Other supramolecular channel structures can be generated by DNA nanotechnologies.[10−13] The DNA nanometer-scale template, built up by triangles organized into a rigid crystalline three-dimensional (3D) lattice with rhombohedral voids (Figure 1L), has been an interesting example of a nanostructure that may hold proteins inside of the pores.[11] It has been designed to help solve protein structures by means of

Received: November 7, 2011
Accepted: January 11, 2012
Published: January 24, 2012

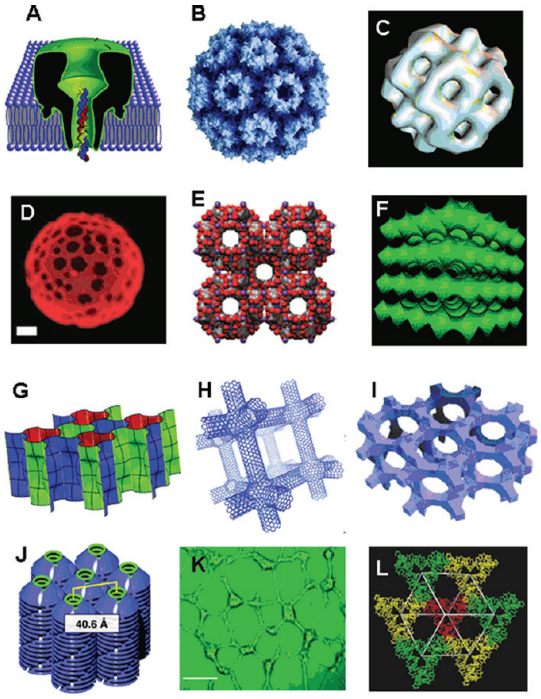

Figure 1. Open-channel architectures generated by self-assembly of proteins, lipids, peptides, polymers, and DNA or by templating of nanoscale building blocks. (A) Heptameric channel protein (α-hemolysin) assembled into a planar lipid bilayer with a linear collagen-like peptide traversing the 1.5 nm diameter pore (reprinted from ref 4). (B) 3D reconstruction of the *cowpea chlorotic mottle virus* (CCMV) (PDB code: 1cwp). The capsid nanoparticle, generated by the protein self-assembly,[32] has a diameter of 28 nm and displays open channels. (C) Liquid-crystalline lipid nanoparticle with an inner cubic lattice organization and a diameter of 58 nm (reprinted from ref 43). (D) Controlled coarsening of polymer vesicles. Scale bar: 2 μm (Reprinted by permission from Macmillan Publishers Ltd.: *Nature Materials* (ref 33), copyright 2009). (E) Nanostructure of cyclodextrin channels (reproduced by permission of John Wiley & Sons Inc. (ref 47), copyright 2010). (F) Bicontinuous double-diamond cubic membrane (crystallographic space group *Pn3m*). The diameter of the aqueous channels is 5.9 nm (determined in ref 46). (G) Triply periodic modulated hexagonal honeycomb pattern of soft channels (reproduced by permission of the Royal Society of Chemistry (ref 34), copyright 2009). (H) Carbon nanotube network forming a channel architecture (reproduced by permission of the Royal Society of Chemistry (ref 49), copyright 2011). (I) Extra-large-pore zeolite framework (reproduced by permission of John Wiley & Sons Inc. (ref 40), copyright 2010). (J) Peptidic macrocycles organized in hexagonally packed helical channels. The estimated pore diameter is 0.4 nm (reprinted from ref 42). (K) Optical micrograph of a green-fluorescent tube network fabricated by hierarchical self-assembly of polymer vesicles. Scale bar: 50 μm (reprinted from ref 41). (L) Nanochannel structure built up by DNA triangles organized into a crystalline 3D lattice with rhombohedral voids (Reprinted by permission from Macmillan Publishers Ltd.: *Nature* (ref 11), copyright 2009).

X-ray crystallography. Furthermore, DNA cages and self-assembled tetrahedra have been proposed as delivery vehicles for proteins.[12] In this approach, the efficiency of the protein transport and delivery would not be very high as every protein molecule requires a separate DNA nano-object carrier. However, the protein protection against enzymatic degradation can be expected to be improved.

This Perspective is devoted to nanochannel materials other than covalent channeled crystals, rigid DNA nanostructures, carbon nanotube bundles and networks, metal−organic frameworks (MOFs), zeolites, surfactant-templated porous silica spheres, porous calcium phosphate ceramics derived via biomimetic mineralization, porous titanium fiber mesh scaffolds, and so forth. These solid-like nanostructures have been classified as porous networks, porous scaffolds, porous materials, and porous media. For MOF materials, the pores diameters have generally been rather small, on the order of 0.2−0.3 nm. However, strategies of templating are being currently developed to build up periodic structures with larger pores as well as with flexible gyroid channel networks.[37−40]

Self-assembled bicontinuous cubic nanostructures, formed by hydrated lipids and amphiphiles, represent a well-established class of channel-forming liquid-crystalline (LC) media.[14−16] The nanochannel-based mesophases originate from the rich polymorphism of the lipid/water systems.[36,56] Figure 1F shows a channel network architecture with double-diamond cubic lattice symmetry. The inverted bicontinuous cubic membrane that is generated by self-assembly of a nonlamellar lipid in excess water medium is characterized by a large surface area-to-volume ratio.[46] It combines swelling capacity with an inner periodicity of a 3D channel network structure. An intrinsic property of the bicontinuous double-diamond cubic membrane is the presence of two intertwined networks of nanochannels. One of them is closed, while the other is open to the external aqueous medium.[36] The fragmentation of the cubic phase (Figure 1F) into particles can yield open-channel nanocontainers exhibiting a double-diamond type unit cell organization (Figure 1C).

The SAXS method is indispensable for distinguishing topologically random channel networks (e.g., bicontinuous sponge phases) from tubular-type or periodically organized (e.g., gyroid) bicontinuous LC structures of aqueous channels.

Small-angle X-ray (SAXS) and neutron (SANS) scattering[68−118] are powerful structural methods for establishing the crystallographic space group symmetry and domain topologies of organized nanochannel systems as determined by the materials properties (Figure 1). The SAXS method is indispensable for distinguishing topologically random channel networks (e.g., bicontinuous sponge phases) from tubular-type (Figure 1G) or periodically organized (e.g., gyroid) bicontinuous LC structures of aqueous channels. Recent progress involves also the prediction and the remarkable structural characterization of channel arrangements in triple-network tricontinuous cubic LCs[35] as well as aqueous channel architectures in tricontinuous LC phases.[34]

Time-resolved SAXS[85−94] (TR-SAXS), especially in the millisecond time scale, has been introduced as a modern method for investigation of the phase transitions in amphiphilic mesophases[85−103] as it allows monitoring of the kinetics of stimuli-induced structure conversion processes and the occurrence of

dx.doi.org/10.1021/jz2014727 | J. Phys. Chem. Lett. 2012, 3, 445−457

intermediate phase states. It is important also for the establishment of size-dependent phase behaviors and the elucidation of the mechanisms of nucleation and formation of new phases. The recent SAXS literature on soft amphiphilic systems has emphasized the lack of sufficient knowledge permitting an in-depth understanding of the mechanisms and the kinetics of the structural phase transformations.[85] In the SAXS study of Ikkala and colleagues,[27] the lipid alkyl tails' crystallization has been found to guide the formation of correlated layered structures in self-assembled polypeptide complexes with PEGylated triple-tail lipids. This result has confirmed the importance of the crystallization event in the hierarchical structure control. On the basis of the obtained SAXS data, the order−order transition from oblique to hexagonal columnar morphology has been stated to be reversible.[27] In another study,[103] the gel formation process of unilamellar vesicles, composed of sodium oleate and 1-octanol, has been followed on a mesoscopic scale by means of time-resolved small-angle neutron scattering (TR-SANS) experiments. The time-dependent evolution of the scattering curves in the low-q-range region has served in kinetic analysis of the network architecture ordering. In perspective, it would be interesting to apply this kind of methodology also to drug nanocarriers with soft inner-channel structures.

A major question related to the utilization of nanochanneled advanced functional or biomimetic materials has been the control of the soft channels sizes.[14−16,86] The variation of the channel diameter is of particular importance for the encapsulation, transport, and release of drug molecules through and from the nanostructured soft channels.[119−121] It has been shown[7−9] that cubic LC hydrogels, being 3D channel networks, provide slow migration of oligonucleotides and can successfully serve as nanochanneled media for electrophoresis. The channel's diameter in cubic-phase LC hydrogels can be varied and adjusted by engineering of the soft nanomaterial (lipid, peptide, protein, polymer) composition and also by the applied external stimuli. In this research area, high-resolution SAXS and TR-SAXS studies[68−90] appear to be very essential for the determination of the nanochannel network structural parameters.

The TR-SAXS knowledge about the phase transition kinetics will improve the understanding of the controlled uptake and release of therapeutic molecules from nanochannel-type carriers.

The channel networks in bicontinuous cubic lipid phases appear to be both hydro-responsive and temperature-responsive.[85,95] For nonlamellar lipids, temperature variations cause changes in the lipid membrane curvature and head group hydration. The thermally induced structural alterations in the bicontinuous cubic phase, formed in a self-assembled monoolein/octylglucoside (OG)/water system, have been studied by means of SANS and SAXS.[95] The soft-matter double-diamond cubic architecture has responded by dramatic swelling (D_{Large} cubic structure)[86] upon incorporation of the hydration-enhancing guest component octylglucoside. The aqueous channel diameter, determined by SAXS analysis at low and ambient temperatures, has increased twice, to ∼7 nm, as a result of this hydro response. Figure 2a presents the time-resolved SAXS

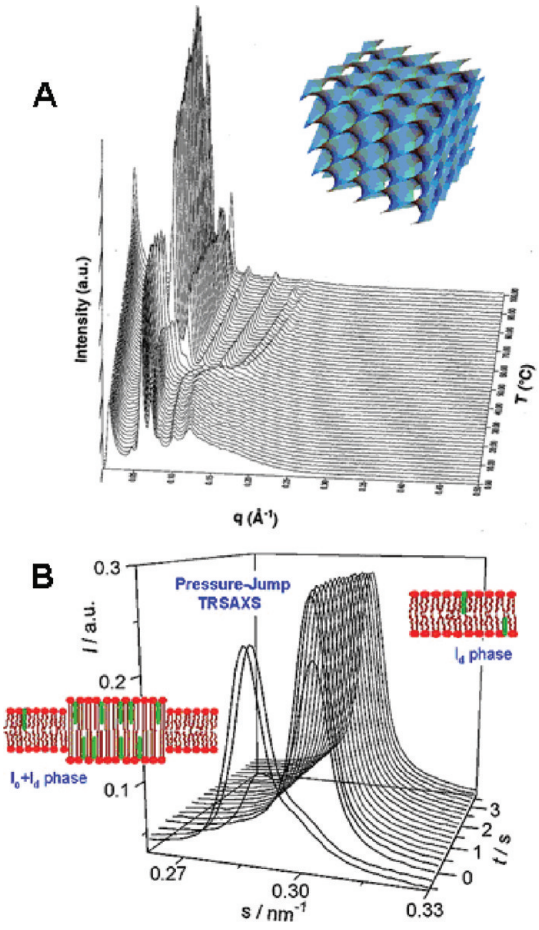

Figure 2. Time-resolved small-angle X-ray scattering (TR-SAXS) patterns of phase transformations in (A) hydrated bicontinuous cubic membranes in the monoolein/octyl glucoside (MO/OG 90/10 mol/mol) self-assembled system showing a swelling, cubic D_{Large}−cubic D_{Normal}, order−order transition between two double-diamond (*Pn3m*) cubic lattices (inset) upon a temperature increase above 40 °C (reprinted from ref 86). (B) A ternary lipid mixture (DOPC/DPPC/Chol 1:2:1), serving as a model system of raftlike membranes, during the first 4 s of a pressure jump from 1.6 to 0.3 kbar at T = 61 °C. The pressure jump, inducing the phase changes, was triggered at t = 0 s (reprinted from ref 100).

patterns recorded during a temperature scan in the interval from 1 to 99 °C. Upon heating, a phase transition has been triggered from the swollen D_{Large} cubic phase to a distinct cubic structure (D_{Normal}) characterized by a different membrane curvature from that of the diamond cubic phase with large water channels.[86] The D_{Normal} cubic phase has displayed a water channel diameter of ∼3 nm. It is anticipated that the diffusion of soluble drug species in the channels of the swollen cubic structure will be enhanced as the permeability of the swollen state to water is higher.

It has been shown that the hydration agent (OG) concentration can be varied as to tune the hydration of the nanochannels in the D_{Large} bicontinuous cubic phase and to control its transformation into a D_{Normal} cubic phase at temperatures above the body temperature.[95] The mechanism of the order−order, D_{Large}−D_{Normal}, structural transition has been related to

dx.doi.org/10.1021/jz2014727 | J. Phys. Chem. Lett. 2012, 3, 445−457

the nanochannel dehydration, domain alignment, and curvature-induced molecular demixing. The established order−order phase transition has been reversible upon cooling.[95] The fact that the release of nanochannel-network-embedded guest molecules can be triggered by the applied temperature stimulus should be further explored in pharmaceutical applications. Toward that aim, additional structural SAXS studies will be required in order to characterize the kinetics of the hydration-dependent phase transitions provoked by the release of different drug compounds.[119,121] Knowledge about the phase transition kinetics will improve the understanding of the controlled uptake and release of therapeutic molecules from nanochannel-type carriers.

On the topic of pressure-jump responsiveness, Winter and colleagues[100] have employed time-resolved SAXS to follow the pressure-jump-induced structural changes in raft membranes of DOPC/DPPC/Chol (1:2:1) as a function of time (Figure 2b). The TR-SAXS patterns have been recorded with a time resolution of 25 ms in order to probe the kinetics of the induced phase transitions from a liquid-disordered (ld) phase to a liquid-ordered (lo)/ld two-phase coexistence region or to a three-phase coexistence region involving solid-ordered (so) phases. The phase transition kinetics from the fluid (ld) phase to the (lo+ld) two-phase coexistence region has been rather rapid. Phases have appeared or disappeared within the 25 ms time resolution of the technique. The authors have brought to mind that the appearance or disappearance of Bragg peaks of phases depends on the cooperativity of many molecules being arranged in a lattice. The measured longer relaxation times have been attributed to the rate-limiting transport and redistribution of water into the new formed phases because the lipid head groups in the different phases are hydrated differently. The TR-SAXS data[100] have revealed that the structural transformations upon bidirectional pressure-jump stimuli are fully reversible and that no intermediate phases have occurred. Despite these very interesting results, temperature- and pressure-jump-coupled TR-SAXS investigations[100,101] still remain scarce.[85] Their potential could be more broadly explored in the area of soft nanochanneled assemblies for biomedical applications.

The potential of temperature-jump-coupled TR-SAXS investigations could be more broadly explored in the area of soft nanochanneled assemblies for biomedical applications.

A recent time-resolved SAXS study[102] has investigated the photoinduced phase changes in a self-assembled system consisting of the surfactant tetraethyleneglycol monodecylether ($C_{10}E_4$), water, *n*-decane, and cyclohexane. Starting from the original phase diagram, phase transitions have been photoinduced from a microemulsion to a bulk LC phase at varying surfactant ($C_{10}E_4$) concentrations and at equal volume fractions of water and oil. Figure 3 shows the time evolution of the SAXS patterns, representing the dynamics of the phase switch from an isotropically oriented solution to a LC state. Before laser illumination, the ternary fluid system has been stabilized at a temperature above 40 °C. Anti-Stokes excitation of embedded dye molecules has served to photoinduce a phase transition, which has led to growth of long-range-order LC domains. The obtained TR-SAXS results have revealed that the exponential nucleation and growth period of the emerging lamellar LC bulk structure is preceded by a concentration-dependent induction time. The macroscopic appearance of the LC phase, formed after optical (laser) excitation of the solution, has been distinct from the one formed after temperature reduction.[102] The possibility for development of this laser-coupled time-resolved X-ray scattering technique to investigate the dynamics of other photoinduced phase transitions, including those in soft channel network self-assembled systems, can be indicated as a perspective.

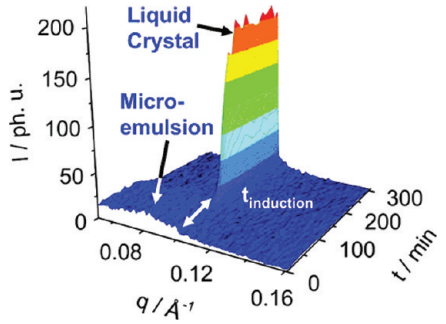

Figure 3. Photoinduced microemulsion/LC phase transition investigated by TR-SAXS with a $C_{10}E_4$/water/*n*-decane/cyclohexane stirred mixture. The photosensitization is done by means of an added dye (Rh101) illuminated by an optical laser with λ = 623.8 nm and p = 3 mW. The increase of the Bragg peak, resulting from the emergence of a lamellar LC structure, occurs after an induction period subsequent to the light illumination at t = 0 min (reprinted from ref 102).

To date, accumulating evidence exists that self-assembly of nonlamellar amphiphiles in liquid medium may produce channeled scaffolds with different architectures and stimuli-responsive features. In fact, amphiphilic LCs, as complex nanostructured fluids, comprise simple "programmable matter" as they may change geometrical shapes, internal architecture, and physicochemical properties in response to external stimuli. The structural and physical properties of LCs could be modulated or modified by application of light, heat, ions, pH changes, ultrasounds, electric or magnetic fields. It has been demonstrated that phase transitions can be induced by photosensitization, temperature changes, pressure jumps, shear stress, and so forth[85−101,104−109,117,118] (Table 1). These possibilities have not been sufficiently explored yet for the design and fabrication of multifunctional nanocarriers with responsiveness to external stimuli.

Examples include (i) stimuli-responsive peptide-conjugated polymer NPs, (ii) biomimetic nanocontainers of self-assembled peptides coupled to PEG chains that bring stealth properties to the stimulus responsiveness and the LC order, and (iii) targeted NPs consisting of magnetic nanoworms and a cyclic peptide (e.g., Cys-Gly-Asn-Lys-Arg-Thr-Arg-Gly-Cys) that binds to a receptor protein on the tumor surface.[27,28,48,51,52,116] Such functionalities help achieve tumor targeting by stimuli-responsive devices decorated by peptide ligands, drug delivery using stimuli-responsive gel networks, hydration-controlled uptake and release of biomolecules, or transport of drugs through chemical labyrinths. It is essential to note that the responsiveness to

dx.doi.org/10.1021/jz2014727 | J. Phys. Chem. Lett. 2012, 3, 445−457

Stimuli-responsive materials, such as thermosensitive, UV-light-responsive, pH-responsive, and magnetic-field-sensitive assemblies, can be engineered to encapsulate and release bioactive compounds for various therapeutic applications.

Table 1. Sample Environment Devices Employed in Dynamic SAXS Investigations of Stimulus-Induced Phenomena or Related Effects

parameter/stimulus-induced process or effect	environment device
hydration/dehydration	vacuum cell or pressure cell
pH change; fluids rapid mixing	stop-flow rapid mixing apparatus
pressure jump	pressure jump cell
temperature shock	temperature control apparatus (Peltier element, heating stage, cryostat)
temperature scan	MICROcaliX device; differential scanning calorimetry
light illumination; photoinduced processes	laser
shear stress	flow cell
elasticity	stretching device
ultrasound effects	ultrasound water bath
magnetic ordering	electromagnet environment
millisecond kinetics	fast shutter and detector
small heterogeneities	micro- and nanobeam device
high throughput sample screening	automated sample changer

external stimuli can be present at different organization levels of supramolecular hierarchy.

pH-responsive self-assembled systems have attracted strong research interest.[112−116] In controlled drug release applications, pH-responsive channels can opened or closed to regulate the supply of therapeutic biomolecules. Recently, stimuli-responsive nanochanneled polymer membranes have been produced by combining self-assembly of flexible (PS-*b*-P4PV) building blocks and a phase inversion technique.[112] A porous membrane structure has been assembled from metal−copolymer micelles subjected to different aqueous environments. Dissolved Cu^{2+} ions have served as promoters of the connectivity between the polyvinylpyridine (P4VP) chains of the different micelles. A highly ordered supramolecular structure of interconnected micelles has been created using these ionic complexing agents (Figure 4). The obtained membrane has very high porosity and a narrow pore size distribution. Its pH-responsive asymmetric nanochannels have diameters in the sub-10 nm range. The performed SAXS analysis has established the ordering of the micelles in 2D morphologies. SAXS has been employed also to characterize the response of the water flux through the membrane at changing pH, which influenced the micelles sizes

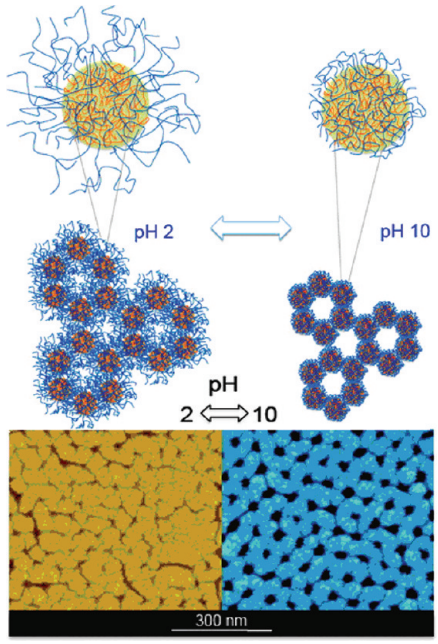

Figure 4. pH-stimuli-responsive soft membranes self-assembled with polymeric micelles in a channel architecture. The micelle size and channel assembly are varied as a function of pH and characterized by SAXS at the Deutsches Elektronen-Synchrotron (DESY) beamline B1 of the DORIS III ring at HASYLAB (Hamburg, DE) (reprinted from ref 112).

and hence the generated channel dimensions (Figure 4). Dramatic reversible volumetric changes have been induced by pH changes between 2 and 10. The pH response of the soft polymer nanochannels has been evidenced as a reversible flux increase of more than 2 orders of magnitude when switching the pH of the aqueous environment of the synthetic pores from 2 to 8.

Using UV light as an external stimulus, advanced light-responsive LC nanocarriers have been designed,[104] aiming at improved on-demand targeting and release. The idea of the authors has been that thermo-sensitive gold-NP-loaded lipid vesicles can release drug content on demand, within a controllable time of light exposure, owing to the enhanced permeability of the lipid membrane during a phase transition. It has been proven that the light-induced L_α−H_{II} phase transition involves alterations in the lipid membrane permeability. Synchrotron radiation TR-SAXS has been used for monitoring of the optothermically induced structural transition of fluid lamellar (L_α) phase DOPE-Me vesicles, loaded with gold NPs, to an inverted hexagonal LC (H_{II}) phase.[104] The TR-SAXS patterns in Figure 5 demonstrate that the absorption of UV light by the gold NPs triggers a fast L_α−H_{II} structural transition in the DOPE-Me NP aqueous dispersion. One minute after switching off the light, the nanostructure retransforms to a vesicular dispersion from the H_{II} phase. It can be suggested in perspective to utilize this UV-activated impact on the lipid membrane permeability for the preparation of stimulus-responsive nanocarriers with controlled drug release properties.

Time-resolved SAXS has been employed also for in situ studies of ion-induced phase transitions of lipid vesicles.[109] Fast structural transformations have been triggered and detected by the combination of a stopped-flow rapid mixing device and in situ SAXS measurements. Figure 6 shows the SAXS patterns obtained after stopped-flow mixing of negatively charged

dx.doi.org/10.1021/jz2014727 | J. Phys. Chem. Lett. 2012, 3, 445−457

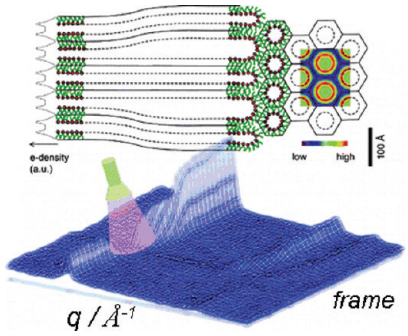

Figure 5. Optothermically induced structural changes in multilamellar lipid vesicles of *N*-methylated dioleoylphosphatidylethanolamine (DOPE-Me) loaded with hydrophilic gold NPs with a size of 4 nm. Synchrotron TR-SAXS experiments (SAXS beamline, ELETTRA, Trieste), combined with UV light source irradiation (λ = 365 nm, EXFO Omnicure S1000 light source), enable establishing of the structure conversion pathway from the fluid lamellar (L_α) phase vesicles to an inverted hexagonal LC (H_{II}) phase through an intermediate state of uncorrelated fluid bilayers during in situ UV activation. The light-induced structural changes appear to be reversible. The exposure time during the UV light experiments is 2 s for each frame (reprinted from ref 104).

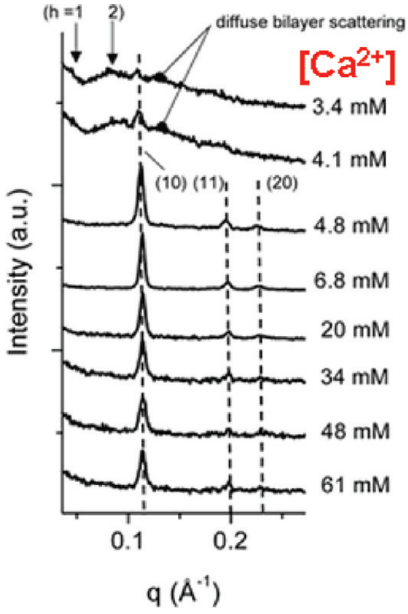

Figure 6. Combined synchrotron SAXS and stopped-flow rapid mixing device technique for in situ monitoring of the calcium ion (Ca^{2+})-induced fast H_{II} phase formation in a DOPG/MO system as a function of the salt concentration. The rapid mixing experiments are carried out at 50 °C using negatively charged DOPG/MO vesicles with a lipid molar ratio of 30/70 (mol/mol). The stopped-flow apparatus allows mixing of the lipid vesicles with a solution of Ca^{2+} ions within 10 ms. The SAXS patterns of the DOPG/MO-based aqueous dispersions (7 wt % lipid) are recorded 71 s after the rapid mixing with the salt solution (the ion concentration $[Ca^{2+}]$ is varied between 3.4 and 61 mM). The Bragg peaks of the H_{II} phase are well-defined at Ca^{2+} concentrations above 4.8 mM, whereas the broad diffuse scattering at lower metal ion concentrations indicates the coexistence with weakly correlated bilayers (reproduced by an Open-Access License from PlosOne (ref 109), copyright 2008).

DOPG/MO (30/70, mol/mol) vesicles and divalent metal cations (Ca^{2+}). Structural transformations have been induced under increasing salt concentration conditions. It has been found that two different cubic phases (*Im3m* and *Pn3m*) could form, under static conditions, upon the addition of Ca^{2+} ions to DOPG/MO multilamellar vesicles. However, under rapid mixing conditions, fast and unexpected bilayer-to-monolayer transition has been observed.[109] The lamellar (L_α) phase has transformed within milliseconds into an inverted hexagonal (H_{II}) phase already at relatively low Ca^{2+} concentrations. A few seconds after the rapid mixing with the Ca^{2+} ions, no further changes in the fully formed H_{II} phase have been detected. Any intermediate structures, eventually formed at ambient temperature, have had short lifetimes (100−400 ms), whereas the formation of intermediate phases has not been detected at all at 50 °C. Such kinds of stopped-flow rapid mixing studies[109] allow one to gain insight into the kinetics and the dynamics of stimuli-induced phase transitions with soft nanocarriers. They should be extended to diverse biochemical systems toward the perspective of characterizing alternative pathways for drug encapsulation and release from stimuli-responsive nanochannel network carriers.

Millisecond structural transformations have been triggered and detected by the combination of a stopped-flow rapid mixing device and in situ SAXS measurements.

Moving forward, novel stimuli-responsive nanostructures and devices can be envisaged from the combination of nanochannel network architectures with stimuli responsiveness. The functionalization of LC assemblies by cyclodextrins (CDs) may produce 3D hierarchical "channel-in-channel" nanostructures. For instance, the incorporation of chemically modified cyclodextrins (Figure 1E), at a controlled lateral density, into self-assembled bicontinuous cubic membranes may yield 3D channel-in-channel multicompartment architectures. The CD ring periphery diameter is around 1.6−1.8 nm, and the CD hydrophobic cavity diameter spans between 0.5 (α-CD) and 0.7 nm (γ-CD). The CD channel array, aligned normally to the lipid bilayer surface, can be anticipated to introduce a new level of hierarchy in the self-assembled channel networks formed in the lipid cubic phase. The hydrophobic cavities of the CD channels can serve for inclusion complexation of guest organic compounds (drugs, fluorophores, diagnostics imaging agents, etc). Figure 7A shows an example of a cyclodextrin nanocarrier building block designed with stimuli-responsive properties.[48,51] The control of the inclusion capacity of the CD channels can be achieved by ring opening or closing upon application of an external chemical stimulus.

On the other hand, the insertion of transmembrane pore proteins (such as porins or ion channels) along the 3D cubic lipid membrane can favor the hierarchical self-assembly of biocompatible channel-in-channel materials. The possibility to control, via external stimuli, the opening−closing of the CD channels (Figure 7A) or the diameter of the transmembrane protein channels (Figures 7B and 1A) indicates new perspectives for the generation of multicompartment nanochanneled stimuli-responsive carriers. The realization of reversible channel

dx.doi.org/10.1021/jz2014727 | J. Phys. Chem. Lett. 2012, 3, 445−457

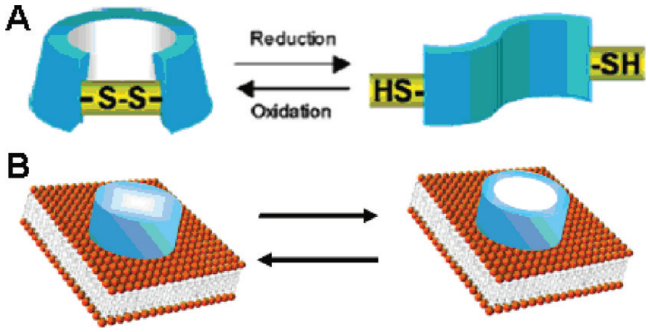

Figure 7. (A) Example of novel stimuli-responsive CD, for which the inclusion ability of the nanochannel can be controlled by the opening or closing of the hydrophobic CD ring based on diethyl−disulfide interconversion. The stimuli-responsive disulfide unit, which is directly inserted into permethylated α- or β-CD skeletons, allows changing of the size and the shape of the CD rings. The chemical yield of cleavage of the S−S bonds with dithiothreitol (DTT) solution, as a reductant, has been higher than 99% at room temperature (reprinted from ref 51). (B) Schematic presentation of closed and open configurations of a stimuli-responsive transmembrane channel protein forming hydrophilic pores in a lipid bilayer membrane. Different kinds of stimuli may open or close the protein channel, for instance, ligand binding (ligand-gated or neurotransmitter-gated channel), mediator regulation (nucleotide-gated channel), selective ion flow (voltage-gated channel), and mechanical stress (mechanically gated channel).

Such innovative stimuli-responsive self-assembled channel architectures may open new roads toward building up of multifunctional carriers for drug delivery and tissue engineering.

swelling/deswelling, channel gating, alteration of the channel diameter, as well as variation of the nanochannel density may provide opportunities for the design of new "breathing" nanomaterials".[84] Evidently, high-resolution structural investigations will be needed for the establishment of their precise 3D network organizations as well as for characterization of the drug transport and release properties of the created channel networks. Studies of the translocation dynamics and pathways of proteins, DNA oligonucleotides, and other therapeutic molecules through networks of straight and kinked channels may initiate new research topics in nanoscience.

Since the 1990s, interest in the preparation of channel-involving LC NPs of nonlamellar amphiphiles[122−155] has grown considerably. Fragmentation of self-assembled bicontinuous cubic lipid phases to NPs, under agitation with biocompatible amphiphilic polymers or PEGylated surfactants, has been a major method for production of cubosome, hexosome, or spongosome types. The optimal dimensions of the lipid NPs for therapeutic and diagnostics purposes are in the range from 50 to 300 nm in diameter. They are being designed as LC nanochanneled containers for loading and release of biomolecular drugs.[119,120] It is known that protein, peptide, and nucleic acid drugs are characterized by low bioavailability that is associated with their poor stability, limited passage through biological barriers, and fast enzymatic degradation. Synthetic LC type nanocarriers[14−16,20,44−46,122−155] have shown promise to overcome some of the problems of recombinant protein and peptide drug instability and rapid elimination.

Inner structures of LC NPs have been determined by means of SAXS.[93,104−108] Among them, the oil-in-water type internally self assembled lipid particles have been referred to as ISAsomes.[93] The SAXS investigations with concentrated dispersions of ISAsomes of monolinolein[84] have reported identical inner structures of the dispersed NPs and the parent bulk nondispersed phases formed at different temperatures. At variance, the comparison of the phase behaviors[152] of fully hydrated nondispersed monoelaidin/water system and that of relatively diluted solutions of dispersed LC NPs has indicated that the *Im3m*−*Pn3m* phase transition temperatures in the two systems differ by about 35 °C. The stabilizing Pluronic F127 polymer has partitioned into the *Pn3m* cubic structure and has favored its transformation into an *Im3m* cubic phase. The lyotropic phase behaviors of glycerol mono-oleate (GMO) and phytantriol-based dispersed NPs systems[147] also have not corresponded to those of the parent nondispersed LC systems. These structural results have suggested that both the amphiphilic dispersing agents and the LC domain size could influence the lattice spacing and symmetry. Generally, the phase behavior of dispersed LC NPs differs from the bulk LC phase behavior.

Detailed SAXS investigations of cubic or hexagonal LC NPs as a function of the number of repeat unit cells inside of the NPs, or as a function of the domain sizes, are still lacking. It is known that Bragg diffraction patterns, resolved with multilamellar lipid vesicles, differ from those of the corresponding nondispersed bulk lamellar LC phases. In fact, the intensity and the width of the SAXS peaks reflect the number of lamellae that built up the multibilayer organization.[108] These effects have not been systematically evaluated yet with channel-based dispersed systems, such as cubosomes and hexosomes. Theoretical simulations should reveal how the SAXS correlation peaks reflect the correlation length of the ordered LC subdomains as well as the disorder induced, for instance, by PEGylation of the lipid membranes in relation to steric stabilization of cubosome NPs with amphiphilic polymers. In perspective, SAXS studies of dispersed LC NPs are anticipated to facilitate the development of new theoretical models,[55] addressing the size dependence of the phase transition temperature in nanoparticulate amphiphilic systems, transport of water, nucleation and crystal growth in nanoparticulate systems, surface-induced melting and other melting-related phenomena, temperature dependence of the interface energy for NP radii varying as a function of the unit cell dimension, and so forth.

Drug release strongly depends on the phase state of the LC nanocarriers at a given temperature.[20,119−121] However, the studies under realistic (patient) conditions are still scarce. The TR-SAXS investigations of the loading and release phenomena from LC NPs, which include confined phase behavior and diffusion in soft nanochanels, constitute an emerging research area. Regarding the water flux in the channels of the dispersed cubic NPs systems, it has been suggested that the water transport should be relatively rapid between the internal core of the mesophase NPs and the external aqueous phase.[147] The high surface-area-to-volume ratio of the cubosome particles supports the hypothesis that the water transport is facilitated is such

dx.doi.org/10.1021/jz2014727 | J. Phys. Chem. Lett. 2012, 3, 445−457

channel-type LC particles, and hence, the drug release will be enhanced as compared to that of impermeable closed particles. Taking into account that the structural organization of the lipid NPs governs their drug release characteristics at a given temperature, several questions may arise from the fact that the lyotropic phase behavior of the dispersed LC nanocarriers significantly differs from that of the corresponding bulk nondispersed phases.[147] For instance, the supercooling effects established with dispersed phytantriol-based NPs (Figure 8)

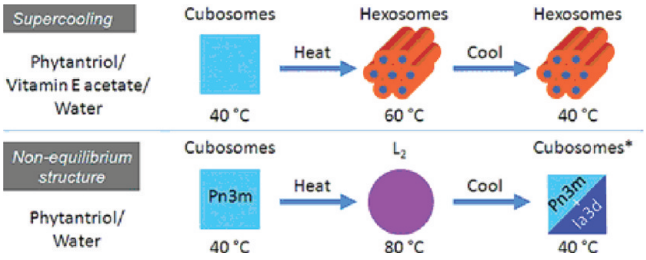

Figure 8. Temperature-induced structural phase sequences determined from SAXS analysis of nanoparticulate LC systems. Differences in the structural phase sequences and in the phase transition temperatures, due to supercooling effects in phytantriol/vitamin E acetate NP systems dispersed in excess water, have been observed with respect to the phytantriol/water dispersion. The SAXS scans have been performed at a rate of 1 °C/min during continuous heating or cooling. The mechanism of phase conversion during cooling differs from that during the heating scan. The lyotropic phase behavior of the dispersed LC NPs significantly differs from that of the corresponding bulk nondispersed phases (adapted from ref 147).

have been greater as compared to those observed with nondispersed LC phases. Additional nonequilibrium phases have appeared on temperature cooling scans.[147] These phenomena indicate the need for further in-dept investigations, by means of SAXS, of the nonequilibrium states during NP structural phase transition and of the size-dependent NP phase behavior.

Moving forward, kinetics studies, by means of time-resolved SAXS,[85] of the mechanisms of nucleation and growth of self-assembled NPs, as well as of their phase transformations, appear to be required for diluted nanoparticulate systems.[104−111] The time evolution and the concentration dependences of the SAXS profiles allow one to establish the pathways of the self-assembly processes and to determine intermediate structures and transient states. Gummel at al.[105] have reported millisecond range kinetics study of the surfactant self-assembly process carried out with the rapid mixing stopped-flow apparatus and TR-SAXS (ESRF, Grenoble). This methodology has permitted the investigation of the morphological transition pathways during the formation of self-assembled unilamellar vesicles, with sub-nanometer structural resolution and a millisecond time resolution. The employed surfactant solutions are comprised of the anionic lithium perfluorooctanoate (LPFO) and the zwitterionic tetradecyldimethylamine oxide (TDMAO). Figure 9 shows the time-resolved scattering curves recorded during the spontaneous self-assembly process occurring after mixing. The formation of unilamellar vesicles has passed through a pathway of aggregates with different shapes. Elongated micelles have initially emerged, while torus-like transient intermediate structures have formed at subsequent stages of the process and at higher surfactant concentrations. The kinetics of the nanoaggregates' transformation has been dependent on the surfactant concentrations. The authors[105]

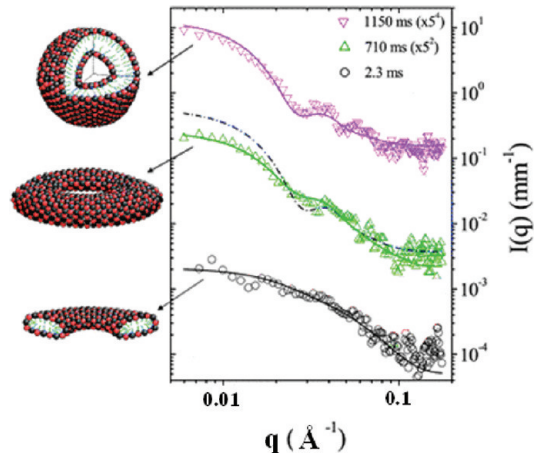

Figure 9. Time evolution of SAXS intensity curves (from t = 2.3 to 1150 ms) in stopped-flow rapid mixing experiments on surfactant self-assembly kinetics using solutions of anionic LPFO and zwitterionic TDMAO. The initial surfactant (8 mM) solutions are rapidly mixed in a ratio TDMAO/LPFO of 3:4 (i.e., at relative mole fraction of x[TDMAO] = 0.43) in order to form self-assembly aggregates with time. The curves have been multiplied by a factor 5 for clarity. The scattering patterns have been fitted with SAXS models for different nanoaggregate shapes (elongated mixed micelles, torus-like micelles, and unilamellar vesicles) presented on the left (reproduced by permission of the Royal Society of Chemistry (ref 105), copyright 2011).

have concluded that similar vesicular final structures can be self-assembled through quite different structural and kinetics pathways. This result appears to be essentially important for the control of the self-assembled nanostructures fabrication.

Structural SAXS studies have accomplished important steps in hierarchical self-assembly design with amphiphilic soft matter and have opened new frontiers in protein and peptide drug delivery.

In conclusion, structural SAXS studies have accomplished important steps in hierarchical self-assembly design with amphiphilic soft matter and have opened new frontiers in protein and peptide drug delivery. LC multifunctional, multidomain, and multicompartment nanocarriers of various architectures and hierarchical organizations are under study. Time-resolved SAXS investigations have been initiated with stimuli-responsive soft materials such as hydrogels and hydro-responsive nanochanneled networks, bioinspired pH-responsive and ion sensitive channels, as well as thermo-responsive, photosensitive, and redox-responsive NPs or channel scaffolds. Dynamic structural studies of stimuli-responsive soft nanochannel structures are anticipated to bring more comprehensive understanding about the triggered release and intracellular delivery from LC nanocarriers using temperature jumps, pH changes, light irradiation,

dx.doi.org/10.1021/jz2014727 | J. Phys. Chem. Lett. 2012, 3, 445−457

rupture by ultrasound waves, electric and magnetic fields, and so forth.

In perspective, the methodologies for dynamic TR-SAXS monitoring of the loading and release phenomena with LC NPs should be further advanced as the research on multicompartment nanocarriers seems to require more rapid progress. The biomolecular translocation and release from soft channel nanofluidics is an emerging subject. Greater understanding of the mechanisms of drug loading and transport and release from nanochannel network carriers may enhance the effectiveness of such drug delivery systems and may contribute to the development of novel controlled release therapeutic devices and intelligent carrier systems for application under more realistic and useful conditions. Novel kinds of channel-in-channel architectures may be designed as representatives of the next-generation breathing soft materials of interpenetrating or interconnected nanochannels.

AUTHOR INFORMATION

Corresponding Author

*E-mail: Angelina.Angelova@u-psud.fr.

Biographies

Angelina Angelova is a CNRS Research Scientist at the UMR8612 Department of Physical Chemistry of Polyphase Systems, Paris-Sud 11 University. She received a Ph.D. degree in Physical Chemistry from the Bulgarian Academy of Sciences, where she was appointed a Research Associate in 1992. After postdoctoral studies at Max-Plank-Institute for Colloids and Interfaces (Berlin) and EMBL (Hamburg), she moved to IMEC (Belgium) in 2000 as a Senior Scientist, and subsequently, she joined CNRS (France) in 2005. Her research interests are in nanostructured multiphase supramolecular amphiphilic assemblies.

Borislav Angelov is a Research Scientist at the Academy of Sciences of the Czech Republic. He received a Ph.D. degree in Biophysics from the Bulgarian Academy of Sciences, where he was appointed a Research Associate in 2002. He was a fellow of the Marie Curie host site Laboratoire de Physique de Solides (LPS Orsay), Paris-Sud 11 University. After a postdoctoral stay at the GKSS Research Centre (Geesthacht, Germany), he continued SAXS investigations at Aarhus University (Denmark) and the Institute of Macromolecular Chemistry (Prague). His research interests include the application of synchrotron radiation techniques to study soft matter nanostructures.

Vasil M. Garamus (Vasyl Haramus) is a scientist in the Department of Structural Research on Macromolecules (HZG, Geesthacht). He received a Ph.D. degree in Physics from Kiev University, Ukraine. He was appointed as a junior researcher at Frank Laboratory of Neutron Physics, (JINR, Dubna, Russia) in 1995. At Helmholtz-Zentrum Geesthacht, he has been responsible for the SANS1 instrument (1998−2010) at reactor FRG-1, and since 2010, he has been co-responsible for the BioSAXS instrument (PETRA III, Hamburg). His research interests are in neutron and X-ray studies of surfactants, polymers, proteins, and NPs in solutions.

Sylviane Lesieur received Ph.D. and Habilitation degrees in Physical Sciences from Université Pierre et Marie Curie (Paris VI). She is a Research Director at CNRS and a head of the Department of Physical Chemistry of Polyphase Systems at UMR8612, Paris-Sud 11 University. Her research interests include magnetic and self-assembled lipid nanocarriers for diagnostics and therapy and studies of the interactions of membrane and cellular models with supramolecular nanoassemblies of lipids.

Patrick Couvreur received a Ph.D. degree in Pharmaceutical Sciences at Université Catholique de Louvain (Belgium). He is a Full Professor of Pharmacy at the Paris-Sud 11 University and a winner of an Advanced ERC grant (EU). He was appointed a Senior Member of the Institut Universitaire de France (IUF) and held a Chair "Innovation Technologique" at the prestigious Collège de France (2009-2010). His research has led to the founding of two start-up companies (BioAlliance Pharma and Medsqual). He is a member of the Academy of Technology, the Academy of Pharmacy, and the Academy of Medicine in France and is a foreign member of the Royal Academy of Medicine in Belgium. Prof. Couvreur is a Leader of the NANO-INNOV project and won the European Pharmaceutical Scientist Award in 2011.

ACKNOWLEDGMENTS

The authors thank Drs. J. S. Pedersen, H. Birkedal, R. Mutafchieva, S. Filippov, U. Vainio, S. Funari, R. Willumeit, C. Bourgaux, P. Štěpánek, and G. Le Bas for continuous cooperation. The programme support "Investissements d'Avenir" (French Ministry of Research and Higher Education) to the LabEx project LERMIT is acknowledged. B.A. acknowledges user support from the Diamond Light Source (Didcot, Oxfordshire, U.K.; Proposal SM3313, Beamline I22), ESRF (Grenoble, France; Proposal SC3113, Beamline ID02), and DESY (Hamburg, Germany; Proposal I-20100216 EC, HASYLAB Beamline B1).

REFERENCES

(1) Cisse, I.; Okumus, B.; Joo, C.; Ha, T. Fueling Protein−DNA Interactions Inside Porous Nanocontainers. *Proc. Natl. Acad. Sci. U.S.A.* **2007**, *104*, 12646−12650.

(2) Xia, D.; Gamble, T. C.; Mendoza, E. A.; Koch, S. J.; He, X.; Lopez, G. P.; Brueck, S. R. J. DNA Transport in Hierarchically-Structured Colloidal-Nanoparticle Porous-Wall Nanochannels. *Nano Lett.* **2008**, *8*, 1610−1618.

(3) Manish, K.; Mariusz Grzelakowski, J. Z.; Clark, Mark; Wolfgang, M. Highly Permeable Polymeric Membranes Based on the Incorporation of the Functional Water Channel Protein Aquaporin Z. *Proc. Natl. Acad. Sci. U.S.A.* **2007**, *104*, 20719−20724.

(4) Todd, C. S.; Long, Y.-T.; Stefureac, R.-I.; Bediako-Amoa, I.; Kraatz, H.-B.; Lee, J. S. Structure of Peptides Investigated by Nanopore Analysis. *Nano Lett.* **2004**, *4*, 1273−1277.

(5) Zhu, X.; Ng, S. Y.; Gupta, A. N.; Feng, Y. P.; Ho, B.; Lapp, A.; Egelhaaf, S. U.; Trevor Forsyth, V.; Haertlein, M.; Moulin, M.; Schweins, R.; van der Maarel., J. R. C. Effect of Crowding on the Conformation of Interwound DNA Strands from Neutron Scattering Measurements and Monte Carlo Simulations. *Phys. Rev. E* **2010**, *81*, 061905.

(6) Osfouri, S.; Stano, P.; Luisi, P. L. Condensed DNA in Lipid Microcompartments. *J. Phys. Chem. B* **2005**, *109*, 19929−19935.

(7) Carlsson, N.; Winge, A. S.; Engström, S.; Åkerman, B. Diamond Cubic Phase of Monoolein and Water as an Amphiphilic Matrix for Electrophoresis of Oligonucleotides. *J. Phys. Chem. B* **2005**, *109*, 18628−18636.

(8) Svingen, R.; Åkerman, B. Mechanism of Electrophoretic Migration of DNA in the Cubic Phase of Pluronic F127 and Water. *J. Phys. Chem. B* **2004**, *108*, 2735−2743.

(9) Carlsson, N.; Sanandaji, N.; Voinova, M.; Åkerman, B. Bicontinuous Cubic Phase of Monoolein and Water as Medium for Electrophoresis of Both Membrane-Bound Probes and DNA. *Langmuir* **2006**, *22*, 4408−4414.

(10) Service, R. F. DNA Nanotechnology Grows Up. *Science* **2011**, *332*, 1140−1143.

(11) Zheng, J.; Birktoft, J. J.; Chen, Y.; Wang, T.; Sha, R.; Constantinou, P. E.; Ginell, S. L.; Mao, C.; Seeman, N. C. From

Molecular to Macroscopic *via* the Rational Design of a Self-Assembled 3D DNA Crystal. *Nature* **2009**, *461*, 74−77.
(12) Erben, C. M.; Goodman, R. P.; Turberfield, A. J. Single-Molecule Protein Encapsulation in a Rigid DNA Cage. *Angew. Chem., Int. Ed.* **2006**, *45*, 7414−7417.
(13) Zhao, Z.; Liu, Y.; Yan, H. Organizing DNA Origami Tiles into Larger Structures Using Preformed Scaffold Frames. *Nano Lett.* **2011**, *11*, 2997−3002.
(14) Clogston, J.; Caffrey, M. Controlling Release from the Lipidic Cubic Phase: Amino Acids, Peptides, Proteins and Nucleic Acids. *J. Controlled Release* **2007**, *107*, 97−111.
(15) Angelova, A.; Angelov, B.; Mutafchieva, R.; Lesieur, S.; Couvreur, P. Self-Assembled Multicompartment Liquid Crystalline Lipid Carriers for Protein, Peptide, and Nucleic Acid Drug Delivery. *Acc. Chem. Res.* **2011**, *44*, 147−156.
(16) Rizwan, S. B.; Boyd, B. J.; Rades, T.; Hook, S. Bicontinuous Cubic Liquid Crystals as Sustained Delivery Systems for Peptides and Proteins. *Expert Opin. Drug Delivery* **2010**, *7*, 1133−1144.
(17) Conn, C. E.; Mulet, X.; Moghaddam, M. J.; Darmanin, C.; Waddington, L. J.; Sagnella, S. M.; Kirby, N.; Varghese, J. N.; Drummond, C. J. Enhanced Uptake of an Integral Membrane Protein, the Dopamine D2L Receptor, by Cubic Nanostructured Lipid Nanoparticles Doped with Ni(II) chelated EDTA Amphiphiles. *Soft Matter* **2011**, *7*, 567−578.
(18) Zabara, A.; Amar-Yuli, I.; Mezzenga, R. Tuning *in-meso*-Crystallized Lysozyme Polymorphism by Lyotropic Liquid Crystal Symmetry. *Langmuir* **2011**, *27*, 6418−6425.
(19) Angelova, A.; Angelov, B.; Papahadjopoulos-Sternberg, B.; Bourgaux, C.; Couvreur, P. Protein Driven Patterning of Self-assembled Cubosomic Nanostructures: Long Oriented Nanoridges. *J. Phys. Chem. B* **2005**, *109*, 3089−3093.
(20) Rizwan, S. B.; Hanley, T.; Boyd, B. J.; Rades, T.; Hook, S. Liquid Crystalline Systems of Phytantriol and Glyceryl Monooleate Containing a Hydrophilic Protein: Characterisation, Swelling and Release Kinetics. *J. Pharm. Sci.* **2009**, *98*, 4191−4204.
(21) Conn, C. E.; Darmanin, C.; Sagnella, S. M.; Mulet, X.; Greaves, T. L.; Varghese, J. N.; Drummond, C. J. Incorporation of the Dopamine D2L Receptor and Bacteriorhodopsin within Bicontinuous Cubic Lipid Phases. 1. Relevance to In-meso Crystallization of Integral Membrane Proteins in Monoolein Systems. *Soft Matter* **2010**, *6*, 4828−4837.
(22) Conn, C. E.; Darmanin, C.; Sagnella, S. M.; Mulet, X.; Greaves, T. L.; Varghese, J. N.; Drummond, C. J. Incorporation of the Dopamine D2L Receptor and Bacteriorhodopsin within Bicontinuous Cubic Lipid Phases. 2. Relevance to In-meso Crystallization of Integral Membrane Proteins in Novel Lipid Systems. *Soft Matter* **2010**, *6*, 4838−4846.
(23) Kamo, T.; Nakano, M.; Kuroda, Y.; Handa, T. Effects of an Amphipathic Alpha-helical Peptide on Lateral Pressure and Water Penetration in Phosphatidylcholine and Monoolein Mixed Membranes. *J. Phys. Chem. B* **2006**, *110*, 24987−24992.
(24) Efrat, R.; Kesselman, E.; Aserin, A.; Garti, N.; Danino, D. Solubilization of Hydrophobic Guest Molecules in the Monoolein Discontinuous Q_L Cubic Mesophase and Its Soft Nanoparticles. *Langmuir* **2009**, *25*, 1316−1326.
(25) Amar-Yuli, I.; Libster, D.; Aserin, A.; Garti, N. Solubilization of Food Bioactives within Lyotropic Liquid Crystalline Mesophases. *Curr. Opin. Colloid Interface Sci.* **2009**, *14*, 21−32.
(26) Angius, R.; Murgia, S.; Berti, D.; Baglioni, P.; Monduzzi, M. Molecular Recognition and Controlled Release in Drug Delivery Systems based on Nanostructured Lipid Surfactants. *J. Phys.: Condens. Matter* **2006**, *18*, S2203−S2220.
(27) Hanski, S.; Junnila, S.; Soininen, A. J.; Ruokolainen, J.; Ikkala, O. Oblique Self-Assemblies and Order−Order Transitions in Polypeptide Complexes with PEGylated Triple-Tail Lipids. *Biomacromolecules* **2010**, *11*, 3440−3447.
(28) Hua, D.; Jiang, J.; Kuang, L.; Jiang, J.; Zheng, W.; Liang, H. Smart Chitosan-Based Stimuli-Responsive Nanocarriers for the Controlled Delivery of Hydrophobic Pharmaceuticals. *Macromolecules* **2011**, *44*, 1298−1302.
(29) Chung, S.-H., Anderson, O. S., Krishnamurthy, V. V., Eds. *Biological Membrane Ion Channels: Dynamics, Structure, and Applications*; Springer: New York, 2007.
(30) Majd, S.; Yusko, E. C.; Billeh, Y. N.; Macrae, M. X.; Yang, J.; Mayer, M. Applications of Biological Pores in Nanomedicine, Sensing, and Nanoelectronics. *Curr. Opin. Biotechnol.* **2010**, *21*, 439−476.
(31) Raunser, S.; Walz, T. Electron Crystallography as a Technique to Study the Structure on Membrane Proteins in a Lipidic Environment. *Annu. Rev. Biophys* **2009**, *38*, 89−105.
(32) Speir, J. A.; Munshi, S.; Wang, G.; Baker, T. S.; Johnson, J. E. Structures of the Native and Swollen Forms of Cowpea Chlorotic Mottle Virus Determined by X-ray Crystallography and Cryo-Electron Microscopy. *Structure* **1995**, *3*, 63−78.
(33) Christian, D. A.; Tian, A.; Ellenbroek, W. E.; Levental, I.; Rajagopal, K.; Janmey, P. A.; Liu, A. J.; Baumgart, T.; Discher, D. E. Spotted Vesicles, Striped Micelles and Janus Assemblies Induced by Ligand Binding. *Nat. Mater.* **2009**, *8*, 843−849.
(34) Hyde, S. T.; de Campo, L.; Oguey, C. Tricontinuous Mesophases of Balanced Three-Arm 'Star Polyphiles'. *Soft Matter* **2009**, *5*, 2782−2794.
(35) Zeng, X. B.; Ungar, G.; Imperor-Clerc, M. A Triple-Network Tricontinuous Cubic Liquid Crystal. *Nat. Mater.* **2005**, *4*, 562−567.
(36) Saksena, R. S.; Coveney, P. V. Self-Assembly of Ternary Cubic, Hexagonal, and Lamellar Mesophases using the Lattice-Boltzmann Kinetic Method. *J. Phys. Chem. B* **2008**, *112*, 2950−2957.
(37) Devic, T.; Horcajada, P.; Serre, C.; Salles, F.; Maurin, G.; Moulin, B.; Heurtaux, D.; Clet, G.; Vimont, A.; Greneche, J.-M.; Le Ouay, B.; Moreau, F.; Magnier, E.; Filinchuk, Y.; Marrot, J.; Lavalley, J.-C.; Daturi, M.; Ferey, G. Functionalization in Flexible Porous Solids: Effects on the Pore Opening and the Host−Guest Interactions. *J. Am. Chem. Soc.* **2010**, *132*, 1127−1136.
(38) Wang, Y.; Li, F. An Emerging Pore-Making Strategy: Confined Swelling-Induced Pore Generation in Block Copolymer Materials. *Adv. Mater.* **2011**, *23*, 2134−2148.
(39) Hsueh, H.-Y.; Chen, H.-Y.; She, M.-S.; Chen, C.-K.; Ho, R.-M.; Gwo, S.; Hasegawa, H.; Thomas, E. L. Inorganic Gyroid with Exceptionally Low Refractive Index from Block Copolymer Templating. *Nano Lett.* **2010**, *10*, 4994−5000.
(40) Jiang, J.; Jorda, J. L.; Diaz-Cabanas, M. J.; Yu, J.; Corma, A. The Synthesis of an Extra-Large-Pore Zeolite with Double Three-Ring Building Units and a Low Framework Density. *Angew. Chem., Int. Ed.* **2010**, *49*, 4986−4988.
(41) Jin, H.; Zhou, Y.; Huang, W.; Yan, D. Polymerization-Like Multilevel Hierarchical Self-Assembly of Polymer Vesicles into Macroscopic Superstructures with Controlled Complexity. *Langmuir* **2010**, *26*, 14512−14519.
(42) Sato, K.; Itoh, Y.; Aida, T. Columnarly Assembled Liquid-Crystalline Peptidic Macrocycles Unidirectionally Orientable over a Large Area by an Electric Field. *J. Am. Chem. Soc.* **2011**, *133*, 13767−13769.
(43) Angelov, B.; Angelova, A.; Papahadjopoulos-Sternberg, B.; Lesieur, S.; Sadoc, J. F.; Ollivon, M.; Couvreur, P. Detailed Structure of Diamond-Type Lipid Cubic Nanoparticles. *J. Am. Chem. Soc.* **2006**, *128*, 5813−5817.
(44) Angelova, A.; Angelov, B.; Papahadjopoulos-Sternberg, B.; Ollivon, M.; Bourgaux, C. Proteocubosomes: Nanoporous Vehicles with Tertiary Organized Fluid Interfaces. *Langmuir* **2005**, *21*, 4138−4143.
(45) Angelova, A.; Angejov, B.; Lesieur, S.; Mutafchieva, R.; Ollivon, M.; Bourgaux, C.; Willumeit, R.; Couvreur, P. Dynamic Control of Nanofluidic Channels in Protein Drug delivery Vehicles. *J. Drug Delivery Sci. Technol.* **2008**, *18*, 41−45.
(46) Angelova, A.; Angelov, B.; Papahadjopoulos-Sternberg, B.; Ollivon, M.; Bourgaux, C. Structural Organization of Proteocubosome Carriers Involving Medium- and Large-Aize Proteins. *J. Drug Delivery Sci. Technol.* **2005**, *15*, 108−112.

(47) Smaldone, R. A.; Forgan, R. S.; Furukawa, H.; Gassensmith, J. J.; Slawin, A. M. Z.; Yaghi, O. M.; Stoddart, J. F. Metal−Organic Frameworks from Edible Natural Products. *Angew. Chem., Int. Ed.* **2010**, *49*, 8630−8634.
(48) Maeda, K.; Mochizuki, H.; Osato, K.; Yashima, E. Stimuli-Responsive Helical Poly(phenylacetylene)s Bearing Cyclodextrin Pendants that Exhibit Enantioselective Gelationin Response to Chirality of a Chiral Amine and Hierarchical Super-Structured Helix Formation. *Macromolecules* **2011**, *44*, 3217−3226.
(49) Varshney, V.; Roy, A. K.; Froudakis, G.; Farmer, B. L. Molecular Dynamics Simulations of Thermal Transport in Porous Nanotube Network Structures. *Nanoscale* **2011**, *3*, 3679−3684.
(50) Song, B.; Yang, J.; Zhao, J.; Fang, H. Intercalation and Diffusion of Lithium Ions in a Carbon Nanotube Bundle by *Ab Initio* Molecular Dynamics Simulations. *Energy Environ. Sci.* **2011**, *4*, 1379−1384.
(51) Kikuzawa, A.; Kida, T.; Akashi, M. Synthesis of Stimuli-Responsive Cyclodextrin Derivatives and Their Inclusion Ability Control by Ring Opening and Closing Reactions. *Org. Lett.* **2007**, *9*, 3909−3912.
(52) Hales, K.; Chen, Z.; Wooley, K. L.; Pochan, D. J. Nanoparticles with Tunable Internal Structure from Triblock Copolymers of PAA-*b*-PMA-*b*-PS. *Nano Lett.* **2008**, *8*, 2023−2026.
(53) Boyd, B. J.; Rizwan, S. B.; Dong, Y.-D.; Hook, S.; Rades, T. Self-Assembled Geometric Liquid-Crystalline Nanoparticles Imaged in Three Dimensions: Hexosomes are not Necessarily flat Hexagonal Prisms. *Langmuir* **2007**, *23*, 12461−12464.
(54) Sagalowicz, L.; Acquistapace, S.; Watzke, H. J.; Michel, M. Study of Liquid Crystal Space Groups using Controlled Tilting with Cryogenic Transmission Electron Microscopy. *Langmuir* **2007**, *23*, 12003−12009.
(55) Dunne, L. J., Manos, G., Eds. *Adsorption and Phase Behaviour in Nanochannels and Nanotubes*; Springer: New York, 2010.
(56) Kaasgaard, T.; Drummond, C. J. Ordered 2-D and 3-D Nanostructured Amphiphile Self-Assembly Materials Stable in Excess Solvent. *Phys. Chem. Chem. Phys.* **2006**, *8*, 4957−4975.
(57) Tiberg, F.; Johnsson, M. Drug Delivery Applications of Non-lamellar Liquid Crystalline Phases and Nanoparticles. *J. Drug Delivery Sci. Technol.* **2011**, *21*, 101−109.
(58) Nazaruk, E.; Bilewicz, R.; Lindblom, G.; Lindholm-Sethson, B. Cubic Phases in Biosensing Systems. *Anal. Bioanal. Chem.* **2008**, *391*, 1569−1578.
(59) Guo, C.; Wang, J.; Cao, F.; Lee, R. J.; Zhai, G. Lyotropic Liquid Crystal Systems in Drug Delivery. *Drug Discovery Today* **2010**, *15*, 1032−1040.
(60) Cashion, M. P.; Long, T. E. Biomimetic Design and Performance of Polymerizable Lipids. *Acc. Chem. Res.* **2009**, *42*, 1016−1025.
(61) Fong, C.; Wells, D.; Krodkiewska, I.; Booth, J.; Hartley, P. G. Synthesis and Mesophases of Glycerate Surfactants. *J. Phys. Chem. B* **2007**, *111*, 1384−1392.
(62) Libster, D.; Aserin, A.; Garti, N. Interactions of Biomacromolecules with Reverse Hexagonal Liquid Crystals: Drug Delivery and Crystallization Applications. *J. Colloid Interface Sci.* **2011**, *356*, 375−386.
(63) Gong, X.; Moghaddam, M. J.; Sagnella, S. M.; Conn, C. E.; Danon, S. J.; Waddington, L. J.; Drummond, C. J. Lyotropic Liquid Crystalline Self-Assembly Material Behavior and Nanoparticulate Dispersions of a Phytanyl Pro-Drug Analogue of Capecitabine-A Chemotherapy Agent. *ACS Appl. Mater. Interfaces* **2011**, *3*, 1552−1561.
(64) Bekkara-Aounallah, F.; Gref, R.; Othman, M.; Reddy, L. H.; Pili, B.; Allain, V.; Bourgaux, C.; Hillaireau, H.; Lepetre-Mouelhi, S.; Desmaele, D.; Nicolas, J.; Chafi, N.; Couvreur, P. Novel PEGylated Nanoassemblies Made of Self-Assembled Squalenoyl Nucleoside Analogues. *Adv. Funct. Mater.* **2008**, *18*, 3715−3725.
(65) Sagalowicz, L.; Leser, M. E. Delivery Systems for Liquid Food Products. *Curr. Opin. Colloid Interface Sci.* **2010**, *15*, 61−72.
(66) Leser, M. E.; Sagalowicz, L.; Michel, M.; Watzke, H. J. Self-assembly of Polar Food Lipids. *Adv. Colloid Interface Sci.* **2006**, *123*, 125−136.
(67) Garg, G.; Saraf, S.; Saraf, S. Cubosomes: An Overview. *Biol. Pharm. Bull.* **2007**, *30*, 350−353.
(68) Angelov, B.; Angelova, A.; Mutafchieva, R.; Lesieur, S.; Vainio, U.; Garamus, V. M.; Jensen, G. V.; Pedersen, J. S. SAXS Investigation of a Cubic to a Sponge (L_3) Phase Transition in Self-Assembled Lipid Nanocarriers. *Phys. Chem. Chem. Phys.* **2011**, *13*, 3073−3081.
(69) Angelov, B.; Angelova, A.; Vainio, U.; Garamus, V. M.; Lesieur, S.; Willumeit, R.; Couvreur, P. Long-Living Intermediates during a Lamellar to a Diamond−Cubic Lipid Phase Transition: A Small-Angle X-ray Scattering Investigation. *Langmuir* **2009**, *25*, 3734−3742.
(70) Yaghmur, A.; Kriechbaum, M.; Amenitsch, H.; Steinhart, M.; Laggner, P.; Rappolt, M. Effects of Pressure and Temperature on the Self-Assembled Fully Hydrated Nanostructures of Monoolein−Oil Systems. *Langmuir* **2010**, *26*, 1177−1185.
(71) Yaghmur, A.; Sartori, B.; Rappolt, M. The Role of Calcium in Membrane Condensation and Spontaneous Curvature Variations in Model Lipidic Systems. *Phys. Chem. Chem. Phys.* **2011**, *13*, 3115−3125.
(72) Persson, G.; Edlund, H.; Amenitsch, H.; Laggner, P.; Lindblom, G. The 1-Monooleoyl-*rac*-glycerol/*n*-Octyl-beta-D-glucoside/Water System. Phase Diagram and Phase Structures Determined by NMR and X-ray Diffraction. *Langmuir* **2003**, *19*, 5813−5822.
(73) Kulkarni, C. V.; Wachter, W.; Iglesias-Salto, G.; Engelskirchen, S.; Ahualli, S. Monoolein: A Magic Lipid? *Phys. Chem. Chem. Phys.* **2011**, *13*, 3004−3021.
(74) Bilalov, A.; Olsson, U.; Lindman, B. DNA−Lipid Self-Assembly: Phase Behavior and Phase Structures of a DNA−Surfactant Complex Mixed with Lecithin and Water. *Soft Matter* **2011**, *7*, 730−742.
(75) Leal, C.; Bouxsein, N. F.; Ewert, K .K.; Safinya, C. R. Highly Efficient Gene Silencing Activity of siRNA Embedded in a Nanostructured Gyroid Cubic Lipid Matrix. *J. Am. Chem. Soc.* **2010**, *132*, 16841−16847.
(76) Leal, C.; Ewert, K. K.; Shirazi, R. S.; Bouxsein, N. F.; Safinya, C. R. Nanogyroids Incorporating Multivalent Lipids: Enhanced Membrane Charge Density and Pore Forming Ability for Gene Silencing. *Langmuir* **2011**, *27*, 7691−7697.
(77) Dong, Y.-D.; Larson, I.; Hanley, T.; Boyd, B. J. Bulk and Dispersed Aqueous Phase Behavior of Phytantriol: Effect of Vitamin E Acetate and F127 Polymer on Liquid Crystal Nanostructure. *Langmuir* **2006**, *22*, 9512−9518.
(78) Hamley, I. W.; Castelletto, V. Small-angle Scattering of Block Copolymers in the Melt, Solution and Crystal States. *Prog. Polym. Sci.* **2004**, *29*, 909−948.
(79) Kulkarni, C. V.; Mezzenga, R.; Glatter, O. Water-in-Oil Nanostructured Emulsions: Towards the Structural Hierarchy of Liquid Crystalline Materials. *Soft Matter* **2010**, *6*, 5615−5624.
(80) Salonen, A.; Guillot, S.; Glatter, O. Determination of Water Content in Internally Self-Assembled Monoglyceride-Based Dispersions from the Bulk Phase. *Langmuir* **2007**, *23*, 9151−9154.
(81) Pili, B.; Bourgaux, C.; Amenitsch, H.; Keller, G.; Lepetre-Mouelhi, S.; Desmaele, D.; Couvreur, P.; Ollivon, M. Interaction of a New Anticancer Prodrug, Gemcitabine-Squalene, with a Model Membrane: Coupled DSC and XRD Study. *Biochim. Biophys. Acta* **2010**, *1798*, 1522−1532.
(82) Shen, H.-H.; Crowston, J. G.; Huber, F.; Saubern, S.; McLean, K. M.; Hartley, P. G. The Influence of Dipalmitoyl Phosphatidylserine on Phase Behaviour of and Cellular Response to Lyotropic Liquid Crystalline Dispersions. *Biomaterials* **2010**, *31*, 9473−9481.
(83) Yaghmur, A.; de Campo, L.; Sagalowicz, L.; Leser, M. E.; Glatter, O. Emulsified Microemulsions and Oil-Containing Liquid Crystalline Phases. *Langmuir* **2005**, *21*, 569−577.
(84) De Campo, L.; Yaghmur, A.; Sagalowicz, L.; Leser, M. E.; Watzke, H.; Glatter, O. Reversible Phase Transitions in Emulsified Nanostructured Lipid Systems. *Langmuir* **2004**, *20*, 5254−5261.
(85) Conn, C. E.; Ces, O.; Mulet, X.; Finet, S.; Winter, R.; Seddon, J. M.; Templer, R. H. Dynamics of Structural Transformations between the Lamellar and Inverse Bicontinuous Cubic Lyotropic Phases. *Phys. Rev. Lett.* **2006**, *96*, 108102.

(86) Angelov, B.; Angelova, A.; Ollivon, M.; Bourgaux, C.; Campitelli, A. Diamond Type Lipid Cubic Phase with Large Water Channels. *J. Am. Chem. Soc.* **2003**, *125*, 7188−7189.
(87) Yaghmur, A.; Laggner, P.; Zhang, S.; Rappolt, M. Tuning Curvature and Stability of Monoolein Bilayers by Designer Lipid-Like Peptide Surfactants. *PloS ONE* **2007**, *2*, e479.
(88) Moitzi, C.; Guillot, S.; Fritz, G.; Salentinig, S.; Glatter, O. Phase Reorganization in Self-Assembled Systems through Interparticle Material Transfer. *Adv. Mater.* **2007**, *19*, 1352−1358.
(89) Lendermann, J.; Winter, R. Interaction of Cytochrome c with Cubic Monoolein Mesophases at Limited Hydration Conditions: The Effects of Concentration, Temperature and Pressure. *Phys. Chem. Chem. Phys.* **2003**, *5*, 1440−1450.
(90) Zhu, Q.; Harris, M. T.; Taylor, L. S. Time-Resolved SAXS/WAXS Study of the Phase Behavior and Microstructural Evolution of Drug/PEG Solid Dispersions. *Mol. Pharm.* **2011**, *8*, 932−939.
(91) Angelova, A.; Ollivon, M.; Campitelli, A.; Bourgaux, C. Lipid Cubic Phases as Stable Nanochannel Network Structures for Protein Biochip Development: X-ray Diffraction Study. *Langmuir* **2003**, *19*, 6928−6935.
(92) Deen, G. R.; Oliveira, C. L. P.; Pedersen, J. S. Phase Behavior and Kinetics of Phase Separation of a Nonionic Microemulsion of $C_{12}E_5$/Water/1-Chlorotetradecane upon a Temperature Quench. *J. Phys. Chem. B* **2009**, *113*, 7138−7146.
(93) Tomsic, M.; Guillot, S.; Sagalowicz, L.; Leser, M. E.; Glatter, O. Internally Self-Assembled Thermoreversible Gelling Emulsions: ISAsomes in Methylcellulose, κ-Carrageenan, and Mixed Hydrogels. *Langmuir* **2009**, *25*, 9525−9534.
(94) Salonen, A.; Muller, F.; Glatter, O. Dispersions of Internally Liquid Crystalline Systems Stabilized by Charged Disklike Particles as Pickering Emulsions: Basic Properties and Time-Resolved Behavior. *Langmuir* **2008**, *24*, 5306−5314.
(95) Angelov, B.; Angelova, A.; Garamus, V. M.; Le Bas, G.; Lesieur, S.; Ollivon, M.; Funari, S. S.; Willumeit, R.; Couvreur, P. Small-angle Neutron and X-ray Scattering from Amphiphilic Stimuli-Responsive Diamond-Type Bicontinuous Cubic Phase. *J. Am. Chem. Soc.* **2007**, *129*, 13474−13479.
(96) Pieranski, P. Thermopermeation in Bicontinuous Lyotropic Crystals. *Liq. Cryst.* **2009**, *36*, 1049−1069.
(97) Guillot, S.; Tomsic, M.; Sagalowicz, L.; Leser, M. E.; Glatter, O. Internally Self-assembled Particles Entrapped in Thermoreversible Hydrogels. *J. Colloid Interface Sci.* **2009**, *330*, 175−179.
(98) Amar-Yuli, I.; Wachtel, E.; Shalev, D. E.; Moshe, H.; Aserin, A.; Garti, N. Thermally Induced Fluid Reversed Hexagonal (H_{II}) Mesophase. *J. Phys. Chem. B* **2007**, *111*, 13544−13553.
(99) Guillot, S.; Moitzi, C.; Salentinig, S.; Sagalowicz, L.; Leser, M. E.; Glatter, O. Direct and Indirect Thermal Transitions from Hexosomes to Emulsified Micro-emulsions in Oil-Loaded Monoglyceride-Based Particles. *Colloids Surf., A* **2006**, *291*, 78−84.
(100) Jeworrek, C.; Pühse, M.; Winter, R. X-ray Kinematography of Phase Transformations of Three-Component Lipid Mixtures: A Time-Resolved Synchrotron X-ray Scattering Study Using the Pressure-Jump Relaxation Technique. *Langmuir* **2008**, *24*, 11851−11859.
(101) Kraineva, J.; Narayanan, R. A.; Kondrashkina, E.; Thiyagarajan, P.; Winter, R. Kinetics of Lamellar-to-Cubic and Intercubic Phase Transitions of Pure and Cytochrome *c* Containing Monoolein Dispersions Monitored by Time-Resolved Small-Angle X-ray Diffraction. *Langmuir* **2005**, *21*, 3559−3571.
(102) Petri, M.; Menzel, A.; Bunk, O.; Busse, G.; Techert, S. Concentration Effects on the Dynamics of Liquid Crystalline Self-Assembly: Time-Resolved X-ray Scattering Studies. *J. Phys. Chem. A* **2011**, *115*, 2176−2183.
(103) Oppel, C.; Prevost, S.; Noirez, L.; Gradzielski, M. The Use of Highly Ordered Vesicle Gels as Template for the Formation of Silica Gels. *Langmuir* **2011**, *27*, 8885−8897.
(104) Yaghmur, A.; Paasonen, L.; Yliperttula, M.; Urtti, A.; Michael Rappolt, M. Structural Elucidation of Light Activated Vesicles. *J. Phys. Chem. Lett.* **2010**, *1*, 962−966.
(105) Gummel, J.; Sztucki, M.; Narayanan, T.; Gradzielski, M. Concentration Dependent Pathways in Spontaneous Self-Assembly of Unilamellar Vesicles. *Soft Matter* **2011**, *7*, 5731−5738.
(106) Narayanan, T. High Brilliance Small-Angle X-ray Scattering Applied to Soft Matter. *Curr. Opin. Colloid Interface Sci.* **2009**, *14*, 409−415.
(107) Vandoolaeghe, P.; Barauskas, J.; Johnsson, M.; Tiberg, F.; Nylander, T. Interaction between Lamellar (Vesicles) and Nonlamellar Lipid Liquid-Crystalline Nanoparticles as Studied by Time-Resolved Small-Angle X-ray Diffraction. *Langmuir* **2009**, *25*, 3999−4008.
(108) Angelov, B.; Angelova, A.; S., K.; Karlsson, G.; Terrill, N.; Lesieur, S.; Štěpánek, P. Topology and Internal Structure of PEGylated Lipid Nanocarriers for Neuronal Transfection: Synchrotron Radiation SAXS and Cryo-TEM Studies. *Soft Matter* **2011**, *7*, 9714−9720.
(109) Yaghmur, A.; Laggner, P.; Sartori, B.; Rappolt, M. Calcium Triggered L_α−H_2 Phase Transition Monitored by Combined Rapid Mixing and Time-Resolved Synchrotron SAXS. *PloS ONE* **2008**, *3*, e2072.
(110) Panine, P.; Finet, S.; Weiss, T. M.; Narayanan, T. Probing Fast Kinetics in Complex Fluids by Combined Rapid Mixing and Small-angle X-ray Scattering. *Adv. Colloid Interface Sci.* **2006**, *127*, 9−18.
(111) Bressel, K.; Muthig, M.; Prévost, S.; Grillo, I.; Gradzielski, M. Mesodynamics: Watching Vesicle Formation in situ by Small-Angle Neutron Scattering. *Colloid Polym. Sci.* **2010**, *288*, 827−840.
(112) Nunes, S. P.; Behzad, A. R.; Hooghan, B.; Sougrat, R.; Karunakaran, M.; Pradeep, N.; Vainio, U.; Peinemann, K.-V. Switchable pH-Responsive Polymeric Membranes Prepared via Block Copolymer Micelle Assembly. *ACS Nano* **2011**, *5*, 3516−3522.
(113) Negrini, R.; Mezzenga, R. pH-Responsive Lyotropic Liquid Crystals for Controlled Drug Delivery. *Langmuir* **2011**, *27*, 5296−5303.
(114) Alam, M. M.; Oka, T.; Ohta, N.; Yamazaki, M. Kinetics of Low pH-Induced Lamellar to Bicontinuous Cubic Phase Transition in Dioleoylphosphatidylserine/Monoolein. *J. Chem. Phys.* **2011**, *134*, 145102−1−145102−10.
(115) Salentinig, S.; Sagalowicz, L.; Glatter, O. Self-Assembled Structures and pK_a Value of Oleic Acid in Systems of Biological Relevance. *Langmuir* **2010**, *26*, 11670−11679.
(116) Knoop, R. J. I.; de Geus, M.; Gijs, J. M.; Habraken, G. J. M.; Koning, C. E.; Menzel, H.; Heise, A. Stimuli Responsive Peptide Conjugated Polymer Nanoparticles. *Macromolecules* **2010**, *43*, 4126−4132.
(117) Porcar, L.; Hamilton, W. A.; Butler, P. D.; Warr, G. G. Scaling of Shear-Induced Transformations in Membrane Phases. *Phys. Rev. Lett.* **2002**, *89*, 168301/1−168301/4.
(118) Mahjoub, H. F.; Bourgaux, C.; Serot, P.; Kleman, M. Evidence of a Sponge-to-Lamellar Phase Transition under Shear by X-ray Scattering Experiments in a Couette Cell. *Phys. Rev. Lett.* **1998**, *81*, 2076−2079.
(119) Boyd, B., J.; Whittaker, D., V.; Khoo, S.-M.; Davey, G. Lyotropic Liquid Crystalline Phases Formed from Glycerate Surfactants as Sustained Release Drug Delivery Systems. *Int. J. Pharm.* **2006**, *309*, 218−226.
(120) Yaghmur, A.; Larsen, S. W.; Schmitt, M.; Østergaard, J.; Larsen, C.; Jensen, H.; Urttib, A.; Rappolt, M. *In situ* Characterization of Lipidic Bupivacaine-Loaded Formulations. *Soft Matter* **2011**, *7*, 8291−8295.
(121) Shah, J. C.; Sadhale, Y.; Chilukuri, D., M. Cubic Phase Gels as Drug Delivery Systems. *Adv. Drug Delivery Rev.* **2001**, *47*, 229−250.
(122) Spicer, P. T. Progress in Liquid Crystalline Dispersions: Cubosomes. *Curr. Opin. Colloid Interface Sci.* **2005**, *10*, 274−279.
(123) Barauskas, J.; Johnsson, M.; Johnson, F.; Tiberg, F. Cubic Phase Nanoparticles (Cubosome): Principles for Controlling Size, Structure, and Stability. *Langmuir* **2005**, *21*, 2569−2577.
(124) Rangelov, S.; Almgren, M. Particulate and Bulk Bicontinuous Cubic Phases Obtained from Mixtures of Glyceryl Monooleate and Copolymers Bearing Blocks of Lipid-Mimetic Anchors in Water. *J. Phys. Chem. B* **2005**, *109*, 3921−3929.

(125) Almgren, M.; Borne, J.; Feitosa, E.; Khan, A.; Lindman, B. Dispersed Lipid Liquid Crystalline Phases Stabilized by a Hydrophobically Modified Cellulose. *Langmuir* **2007**, *23*, 2768−2777.
(126) Almgren, M.; Rangelov, S. Polymorph Dispersed Particles from the Bicontinuous Cubic Phase of Glycerol Monooleate Stabilized by PEG-Copolymers with Lipid-Mimetic Hydrophobic Anchors. *J. Dispersion Sci. Technol.* **2006**, *27*, 599−609.
(127) Murgia, S.; Falchi, A. M.; Mano, M.; Lampis, S.; Angius, R.; Carnerup, A. M.; Schmidt, J.; Diaz, G.; Giacca, M.; Talmon, Y.; Monduzzi, M. Nanoparticles from Lipid-Based Liquid Crystals: Emulsifier Influence on Morphology and Cytotoxicity. *J. Phys. Chem. B* **2010**, *114*, 3518−3525.
(128) Barauskas, J.; Misiunas, A.; Gunnarsson, T.; Tiberg, F.; Johnsson, M. "Sponge" Nanoparticle Dispersions in Aqueous Mixtures of Diglycerol Monooleate, Glycerol Dioleate, and Polysorbate 80. *Langmuir* **2006**, *22*, 6328−6334.
(129) Rosa, M.; Infante, M. R.; Miguel, M. D.; Lindman, B. Spontaneous Formation of Vesicles and Dispersed Cubic and Hexagonal Particles in Amino Acid-Based Catanionic Surfactant Systems. *Langmuir* **2006**, *22*, 5588−5596.
(130) Chong, J. Y. T.; Mulet, X.; Waddington, L. J.; Boyd, B. J.; Drummond, C. J. Steric Stabilisation of Self-Assembled Cubic Lyotropic Liquid Crystalline Nanoparticles: High throughput Evaluation of Triblock Polyethylene Oxide−Polypropylene Oxide−Polyethylene Oxide Copolymers. *Soft Matter* **2011**, *7*, 4768−4777.
(131) Yaghmur, A.; Glatter, O. Characterization and Potential Applications of Nanostructured Aqueous Dispersions. *Adv. Colloid Interface Sci.* **2009**, *147*−*48*, 333−342.
(132) Boyd, B. J.; Dong, Y.-D.; Rades, T. Nonlamellar Liquid Crystalline Nanostructured Particles: Advances in Materials and Structure Determination. *J. Liposome Res.* **2009**, *19*, 12−28.
(133) Uyama, M.; Nakano, M.; Yamashita, J.; Handa, T. Useful Modified Cellulose Polymers as New Emulsifiers of Cubosomes. *Langmuir* **2009**, *25*, 4336−4338.
(134) Salentinig, S.; Yaghmur, A.; Guillot, S.; Glatter, O. Preparation of Highly Concentrated Nanostructured Dispersions of Controlled Size. *J. Colloid Interface Sci.* **2008**, *326*, 211−220.
(135) Amar-Yuli, I.; Wachtel, E.; Ben Shoshan, E.; Danino, D.; Aserin, A.; Garti, N. Hexosome and Hexagonal Phases Mediated by Hydration and Polymeric Stabilizer. *Langmuir* **2007**, *23*, 3637−3645.
(136) Woerle, G.; Drechsler, M.; Koch, M. H. J.; Siekmann, B.; Westesen, K.; Bunjes, H. Influence of Composition and Preparation Parameters on the Properties of Aqueous Monoolein Dispersions. *Int. J. Pharm.* **2007**, *329*, 150−157.
(137) Bryskhe, K.; Schillen, K.; Olsson, U.; Yaghmur, A.; Glatter, O. Formation of Internally Nanostructured Triblock Copolymer Particles. *Langmuir* **2005**, *21*, 8597−8600.
(138) Barauskas, J.; Johnsson, M.; Tiberg, F. Self-assembled Lipid Superstructures: Beyond Vesicles and Liposomes. *Nano Lett.* **2005**, *5*, 1615−1619.
(139) Popescu, G.; Barauskas, J.; Nylander, T.; Tiberg, F. Liquid Crystalline Phases and Their Dispersions in Aqueous Mixtures of Glycerol Monooleate and Glyceryl Monooleyl Ether. *Langmuir* **2007**, *23*, 496−503.
(140) Sagalowicz, L.; Michel, M.; Adrian, M.; Frossard, P.; Rouvet, M.; Watzke, H. J.; Yaghmur, A.; De Campo, L.; Glatter, O.; Leser, M. E. Crystallography of Dispersed Liquid Crystalline Phases Studded by Cryo-Transmission Electron Microscopy. *J. Microscopy* **2006**, *221*, 110−121.
(141) Yaghmur, A.; de Campo, L.; Salentinig, S.; Sagalowicz, L.; Leser, M. E.; Glatter, O. Oil-Loaded Monolinolein-Based Particles with Confined Inverse Discontinuous Cubic Structure (*Fd3m*). *Langmuir* **2006**, *22*, 517−521.
(142) Sagalowicz, L.; Leser, M. E.; Watzke, H. J.; Michel, M. Monoglyceride Self-Assembly Structures as Delivery Vehicles. *Trends Food Sci. Technol.* **2006**, *17*, 204−214.
(143) Yang, D.; Armitage, B.; Marder, S. R. Cubic Liquid-Crystalline Nanoparticles. *Angew. Chem., Int. Ed.* **2004**, *43*, 4402−4409.
(144) Kamo, T.; Nakano, M.; Leesajakul, W.; Sugita, A.; Matsuoka, H.; Handa, T. Nonlamellar Liquid Crystalline Phases and their Particle Formation in the Egg Yolk Phosphatidylcholine/Diolein System. *Langmuir* **2003**, *19*, 9191−9195.
(145) Fraser, S.; Separovic, F.; Polyzos, A. Cubic Phases of Ternary Amphiphile−Water Systems. *Eur. Biophys. J. Biophys. Lett.* **2009**, *39*, 83−90.
(146) Esposito, E.; Eblovi, N.; Rasi, S.; Drechsler, M.; Di Gregorio, G. M.; Menegatti, E.; Cortesi, R. Lipid-Based Supramolecular Systems for Topical Application: A Preformulatory Study. *AAPS PharmSci.* **2003**, *5*, e30.
(147) Dong, Y.-D.; Tilley, A. J.; Larson, I.; Lawrence, M.; J. Amenitsch, H.; Rappolt, M.; Hanley, T.; Boyd, B. J. Nonequilibrium Effects in Self-Assembled Mesophase Materials: Unexpected Supercooling Effects for Cubosomes and Hexosomes. *Langmuir* **2010**, *26*, 9000−9010.
(148) Worle, G.; Siekmann, B.; Koch, M. H. J.; Bunjes, H. Transformation of Vesicular into Cubic Nanoparticles by Autoclaving of Aqueous Monoolein/Poloxamer Dispersions. *Eur. J. Pharm. Sci.* **2006**, *27*, 44−53.
(149) Salonen, A.; Moitzi, C.; Salentinig, S.; Glatter, O. Material Transfer in Cubosome-Emulsion Mixtures: Effect of Alkane Chain Length. *Langmuir* **2010**, *26*, 10670−10676.
(150) Yaghmur, A.; de Campo, L.; Sagalowicz, L.; Leser, M. E.; Glatter, O. Control of the Internal Structure of MLO-Based Isasomes by the Addition of Diglycerol Monooleate and Soybean Phosphatidylcholine. *Langmuir* **2006**, *22*, 9919−9927.
(151) Guillot, S.; Salentinig, S.; Chemelli, A.; Sagalowicz, L.; Leser, M. E.; Glatter, O. Influence of the Stabilizer Concentration on the Internal Liquid Crystalline Order and the Size of Oil-Loaded Monolinolein-Based Dispersions. *Langmuir* **2010**, *26*, 6222−6229.
(152) Yaghmur, A.; Laggner, P.; Almgren, M.; Rappolt, M. Self-Assembly in Monoelaidin Aqueous Dispersions: Direct Vesicles to Cubosomes Transition. *PloS ONE* **2008**, *3*, e3747.
(153) Muller, F.; Salonen, A.; Glatter, O. Monoglyceride-based Cubosomes Stabilized by Laponite: Separating the Effects of Stabilizer, pH and Temperature. *Colloids Surf., A* **2010**, *358*, 50−56.
(154) Muller, F.; Salonen, A.; Glatter, O. Phase Behavior of Phytantriol/Water Bicontinuous Cubic *Pn3m* Cubosomes Stabilized by Laponite Disc-Like Particles. *J. Colloid Interface Sci.* **2010**, *342*, 392−398.
(155) Salonen, A.; Muller, F.; Glatter, O. Internally Self-Assembled Submicrometer Emulsions Stabilized by Spherical Nanocolloids: Finding the Free Nanoparticles in the Aqueous Continuous Phase. *Langmuir* **2010**, *26*, 7981−7987.